Journal of Physics: Conference Series

Markov Processes in Image Processing

Markov Processes in Image Processing

E P Petrov, N L Kharina

Vyatka State University, 36, Moskovskaya St., Kirov, 610000, Russia

E-mail: Eppetrov@mail.ru

Abstract. Digital images are used as an information carrier in different sciences and technologies. The aspiration to increase the number of bits in the image pixels for the purpose of obtaining more information is observed. In the paper, some methods of compression and contour detection on the basis of two-dimensional Markov chain are offered. Increasing the number of bits on the image pixels will allow one to allocate fine object details more precisely, but it significantly complicates image processing. The methods of image processing do not concede by the efficiency to well-known analogues, but surpass them in processing speed. An image is separated into binary images, and processing is carried out in parallel with each without an increase in speed, when increasing the number of bits on the image pixels. One more advantage of methods is the low consumption of energy resources. Only logical procedures are used and there are no computing operations. The methods can be useful in processing images of any class and assignment in processing systems with a limited time and energy resources.

1. Introduction

Now digital images (DI) are used as an information carrier in different sciences and technologies. For a human eye, a 24-bit representation of a color DI is optimal. In different sciences and technologies, the aspiration to increase the number of bits on the DI pixels for the purpose of obtaining more information is observed. For example, having increased the number of bits on the DI pixels of space, medical pictures, pictures in control systems, it is possible to find and recognize more precisely the objects of interest or the controlled process. Increasing the number of bits on the DI pixels will allow one to allocate fine object details more precisely, but it significantly complicates image processing. For the transmission and storage of multidigit DI, the all known algorithms of compression, such as JPEG, JPEG2000, are not always applicable [1-6]. Another important task is the detection of objects interest. Most common methods are those on the Roberts, Previtt and Sobel operators. The main shortcomings of these methods are high sensitivity to noise, a possibility of emergence of gaps in a contour and absence of vagueness on the edge. The Canny method allows one to define correctly the position of edges, but it is the complicated in realization [1, 2, 7].

The choice of the method depends on an ultimate goal of image processing, a type of the images, available computing capacities.

In the paper, methods of compression and edge detection are offered on the basis of two-dimensional Markov chain. The methods are simple in realization, allowing one to process images of more than 24 bits on a pixel.

2. Method description

Let us assume that g-bit DI is represented as a two-dimension Markov process with the number of conditions $N = 2^g$, initial probabilities vector $P = \|p_1, p_2, ..., p_N\|^T$ and transition from state M_i to neighbour state M_j $(i, j \in N)$ of probability matrixes (TPM) ${}^1\Pi$ and ${}^2\Pi$, horizontally and vertically respectively [3]:

$$ {}^1\Pi = \begin{Vmatrix} {}^1\pi_{11} & {}^1\pi_{12} & \dots & {}^1\pi_{1N} \\ {}^1\pi_{21} & {}^1\pi_{22} & \dots & {}^1\pi_{2N} \\ \dots & \dots & \dots & \dots \\ {}^1\pi_{N1} & {}^1\pi_{N2} & \dots & {}^1\pi_{NN} \end{Vmatrix}, \quad {}^2\Pi = \begin{Vmatrix} {}^2\pi_{11} & {}^2\pi_{12} & \dots & {}^2\pi_{1N} \\ {}^2\pi_{21} & {}^2\pi_{22} & \dots & {}^2\pi_{2N} \\ \dots & \dots & \dots & \dots \\ {}^2\pi_{N1} & {}^2\pi_{N2} & \dots & {}^2\pi_{NN} \end{Vmatrix}. \tag{1} $$

With such representation, the development of the DI processing method requires large computational resources especially for images with high bit count (g>8 for each color component). That is why it is essential to split g-bit DI into g binary images (BI).

The splitting procedure is represented in fig. 1.

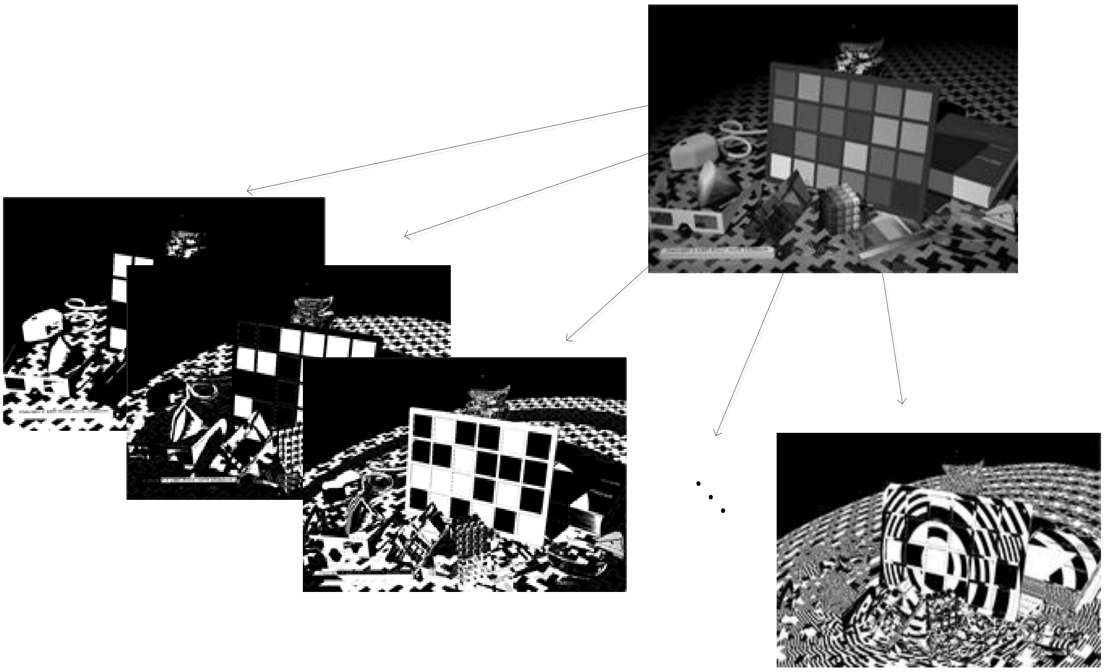

Figure 1. Splitting DI into BI

Each BI is represented as a two-dimensional Markov chain with two (N = 2) equiprobable states $(p_1 = p_2)$ and there is a horizontal and vertical transition from state M_i to neighbour state M_j $(i, j \in N)$ TPM ${}^1\Pi$ and ${}^2\Pi$ respectively [3]:

$$ {}^1\Pi = \begin{Vmatrix} {}^1\pi_{11} & {}^1\pi_{12} \\ {}^1\pi_{21} & {}^1\pi_{22} \end{Vmatrix}, \quad {}^2\Pi = \begin{Vmatrix} {}^2\pi_{11} & {}^2\pi_{12} \\ {}^2\pi_{21} & {}^2\pi_{22} \end{Vmatrix}. \tag{2} $$

TPMs' elements (2) meet the following normalization and stationarity condition:

$$ \sum_{j=1}^{N} {}^q\pi_{ij} = 1,\ i \in N,\ q = \overline{1,2}\ ; \tag{3} $$

$$p_i = \sum_{j=1}^{N} p_j \pi_{ij},\ i \in N\ . \tag{4}$$

BI is represented as random Markov field on an asymmetric half-plane, obtained by the classical scanning from upper left down to left and right (fig. 2).

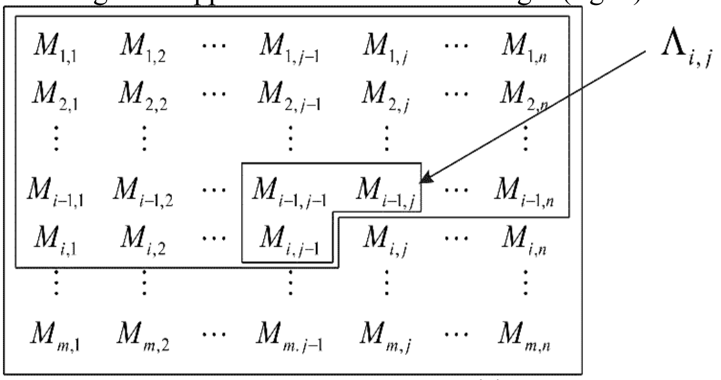

Figure 2. BI model

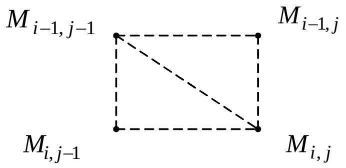

Figure 3. The neighborhood of the predicted BI element

The $M_{i,j}$ $(i \in m, j \in n)$ elements' state depends only on known elements in some subset $\Lambda_{i,j}$. It is the neighbourhood of element $M_{i,j}$. The configuration of the surroundings that meets the condition of causality best of all is the following (fig. 3) [3]:

$$\Lambda_{i,j} = \{M_{i,j-1}, M_{i-1,j}, M_{i-1,j-1}\}. \tag{5}$$

Probabilities of transition from elements $\Lambda_{i,j}$ state to state $M_{i,j}$ form the following TPM:

$$\Pi = \begin{Vmatrix} \pi_{111} & \pi_{121} & \pi_{211} & \pi_{221} \\ \pi_{112} & \pi_{122} & \pi_{212} & \pi_{222} \end{Vmatrix}^T . \tag{6}$$

Matrix Π elements (6) are associated with TPM elements (2) as follows:

$$\pi_{111} = \frac{{}^1\pi_{11} \cdot {}^2\pi_{11}}{{}^3\pi_{11}},\ \pi_{112} = \frac{{}^1\pi_{12} \cdot {}^2\pi_{12}}{{}^3\pi_{11}},\ \pi_{121} = \frac{{}^1\pi_{11} \cdot {}^2\pi_{21}}{{}^3\pi_{12}},\ \pi_{122} = \frac{{}^1\pi_{12} \cdot {}^2\pi_{22}}{{}^3\pi_{12}},$$

$$\pi_{211} = \frac{{}^1\pi_{21} \cdot {}^2\pi_{11}}{{}^3\pi_{21}},\ \pi_{212} = \frac{{}^1\pi_{21} \cdot {}^2\pi_{12}}{{}^3\pi_{21}},\ \pi_{221} = \frac{{}^1\pi_{21} \cdot {}^2\pi_{21}}{{}^3\pi_{22}},\ \pi_{222} = \frac{{}^1\pi_{22} \cdot {}^2\pi_{22}}{{}^3\pi_{22}},$$

where ${}^3\pi_{ii}$ is the elements of TPM ${}^3\Pi = {}^1\Pi \times {}^2\Pi'$.

The proposed methods are based on the procedure of prediction each BI element state using the known neighborhood $\Lambda_{i,j}$ and TPM (6). The procedure of prediction forms BI as follows: if pixel state is predicted correctly, its state in BI is "zero", otherwise it is "one". During BI restoration, "zero" pixels are replaced by predicted states, and those incorrectly predicted (with state "one") are replaced with inversion of the predicted states.

Formal description of the algorithm predictions is the following [4,5]:

1. For each BI, TPM (2) and (6) are calculated.
2. Element $\hat{M}_{ij}$ is predicted based on TPM (6) and neighborhood $\Lambda_{i,j}$.
3. If $M_{ij} = \hat{M}_{ij}$, then element is predicted correctly.
4. If $M_{ij} \neq \hat{M}_{ij}$, then element M_{ij} is predicted incorrectly.

The DI compression method includes splitting into BI, prediction and coding and it works in lossless and lossy modes.

Formal description of the compression algorithm predictions is the following [8]:

1. DI is split into g BI.
2. BI is formed after prediction.
3. BI is compressed with RLE into one-dimensional flow.
4. One-dimensional flow is compressed with Huffman code.

Compressed data are written to a file.

3. EXPERIMENTAL RESULTS

Comparison with the best-known compression algorithms (such as PNG, JPEG-LS, JPEG and JPEG 2000) helps to examine the effectiveness of the proposed algorithm. More than 100 DI of different types were used to get statistics for comparison. Test images compression results using the proposed algorithm and analogues are shown in fig. 4,5 and table 1.

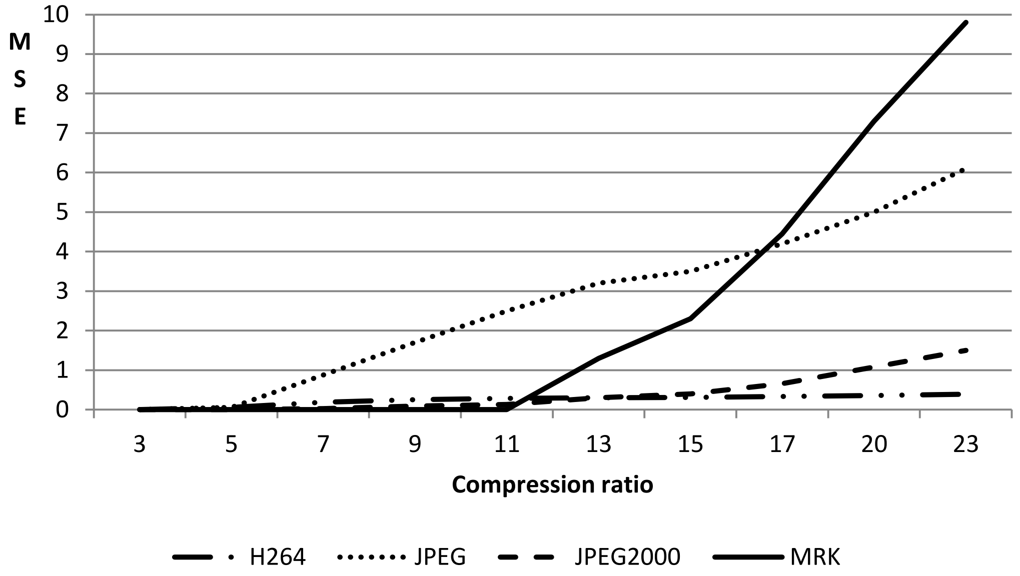

Figure 4. Compression results

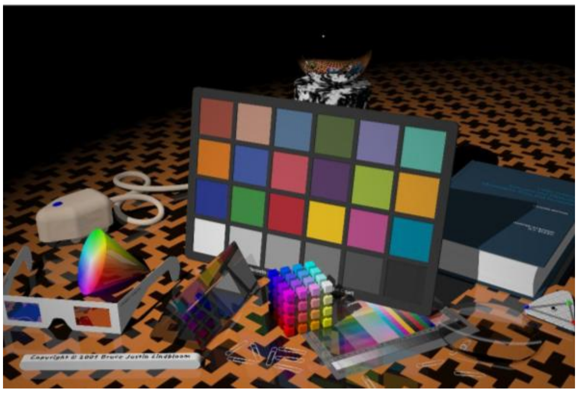

Figure 5a. The test image

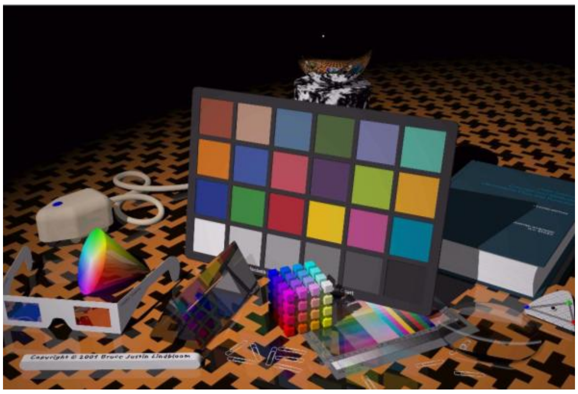

Figure 5b. Compressed image with compression ratio 18 (MSE 9,8)

Table 1. Compression algorithms analysis

Compression algorithm	*Compression ratio*	*Processing speed, Mbs*
PNG	1.86	3.72
JPEG-LS	1.95	15.67
JPEG 2000	1.78	3.88
MRK	1.75	41.8

Formal description of the edge detection algorithm is the following [9]:
1. DI is split into g BI.
2. For 2-3 senior BI prediction procedure is performed.
3. DI image edge is detected.

To research the effectiveness of the proposed algorithm, the test image fig. 6a) and edge detecting results with the use of Roberts (fig. 6b), Prewitt (fig. 6c), Sobel (fig. 6d) and proposed methods (fig. 4e) were taken. In table 2, results of processing speed are shown.

Figure 6a. Test image

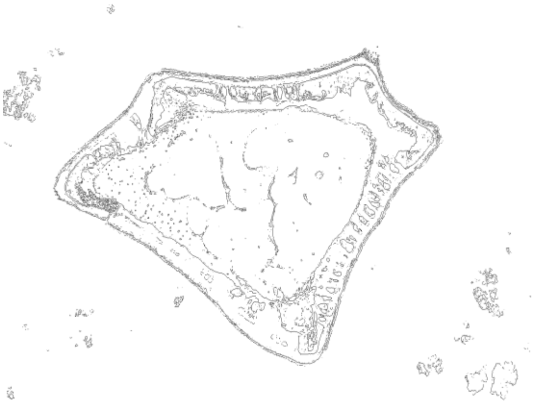

Figure 6b. The edge detected by the Roberts operator

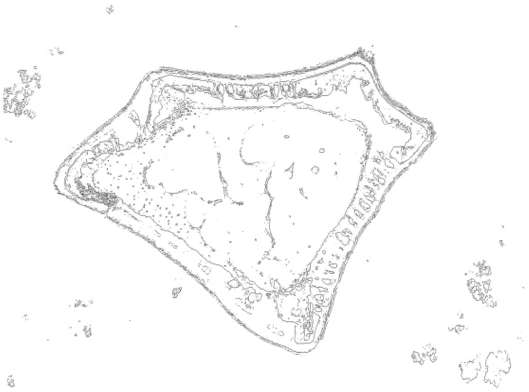

Figure 6c. The edge detected by the Prewitt operator

Figure 6e. The edge detected with the use of the proposed method

Table 2. Edge detector algorithms analysis

Edge detector algorithms	*Processing speed, Mbs*
Roberts	739
Prewitt	549
Sobel	519
Canny	181
Proposed method	1131

4. Conclusion
The proposed image processing methods are not less effective compared with the well-known analogue, but exceed them in processing speed due to splitting the image into BI and simultaneous processing. Methods allow image processing without speed increasing with higher DI bit count. Another advantage of the methods is indiscriminateness to energy resources since the implementation comprises only a logical procedure and there is no computing. Methods can be useful for processing the images of any class and assignment in processing systems with a limited time and energy resources.

References
[1] Gonzalez R and Woods R 2002 *Digital image processing* 813
[2] Jahne B 2005 *Digital image processing* 639
[3] Sullivan G J, Ohm J, Han W-J, and Wiegand T 2012 *IEEE Trans. Circuits* **22(12)** 1649–1668
[4] Lainema J, Bossen F., Han W-J, Min J, and Ugur K 2012 *IEEE Trans. Circuits* **22(12)** 1792–1801
[5] Saxena A and Fernandes F C 2013 *IEEE Trans. Image Process* **22(10)** 3974–3981
[6] Kamisli F 2015 *IEEE Trans. Image Process* **24(4)** 1247-1260
[7] Ivanov E S 2016 *Current problems in remote sensing of the Earth from space* **1** 105-116
[8] Petrov E P, Kharina N L and Sukhikh P N 2016 *Current problems in remote sensing of the Earth from space* **2** 203-210
[9] Petrov E P, Kharina N L and Chukaev K N 2016 *Current problems in remote sensing of the Earth from space* **5** 304-31